Supporting Information

2-pyridine cyclic triimidazole as chelating and bridging ligand in mono- and hexanuclear Re(I) complexes with emissive properties in solution and in the solid state

Daniele Malpicci,[a] Daniele Maver,[a] Daniela Maggioni,[a,b] Pierluigi Mercandelli,[a] Lucia Carlucci,[a,b] Elena Cariati,[a,b] Patrizia Mussini,[a] Monica Panigati*[a,b]

[a] *Dipartimento di Chimica, Università degli Studi di Milano, Via Golgi 19, 20133 Milano (Italy)*

[b] *Consorzio INSTM, Via G. Giusti 9, 50121 Firenze, Italy.*

List of Contents

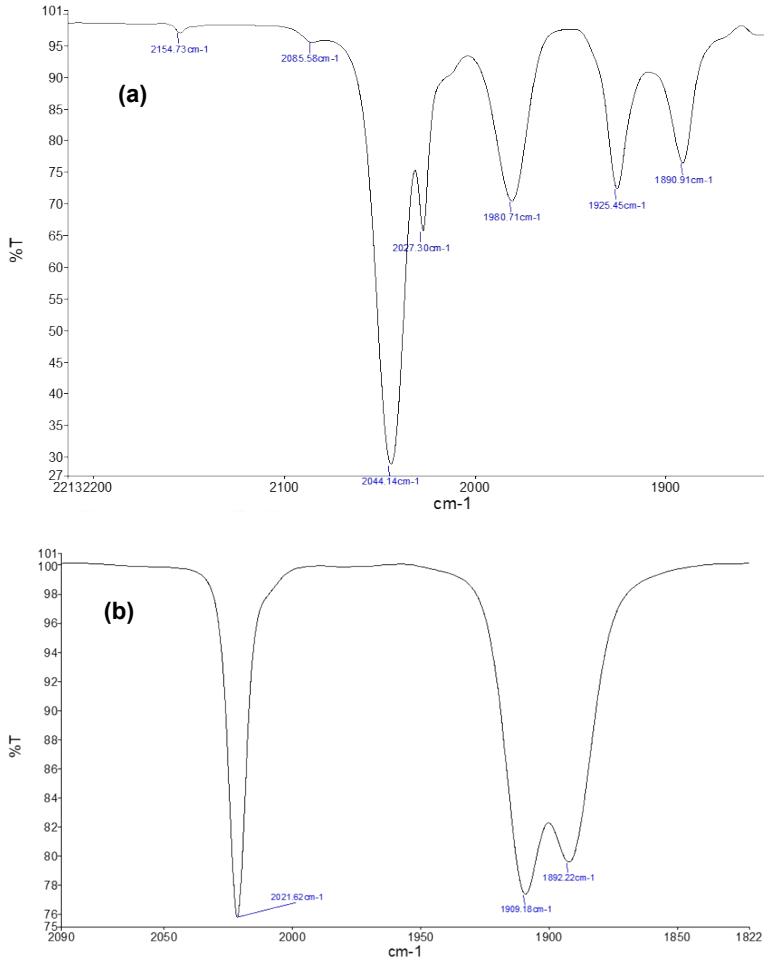

Figure S1: FTIR monitoring of formation of complex **1** (a) after 5 minutes (b) at the end of reaction, in toluene solution.

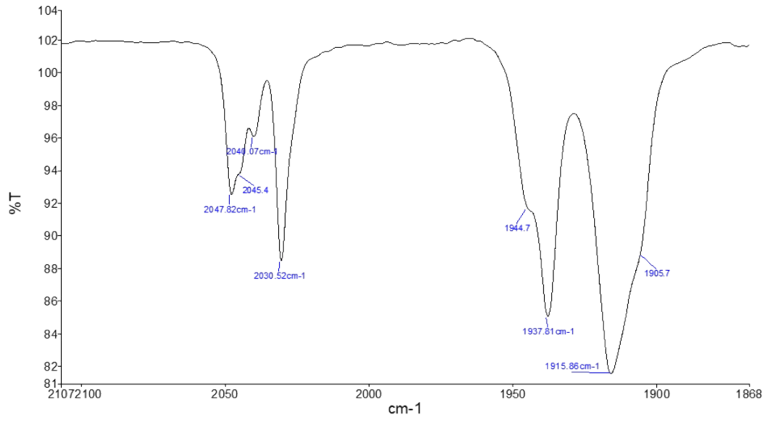

Figure S2: FTIR spectra of complex **2** in toluene solution

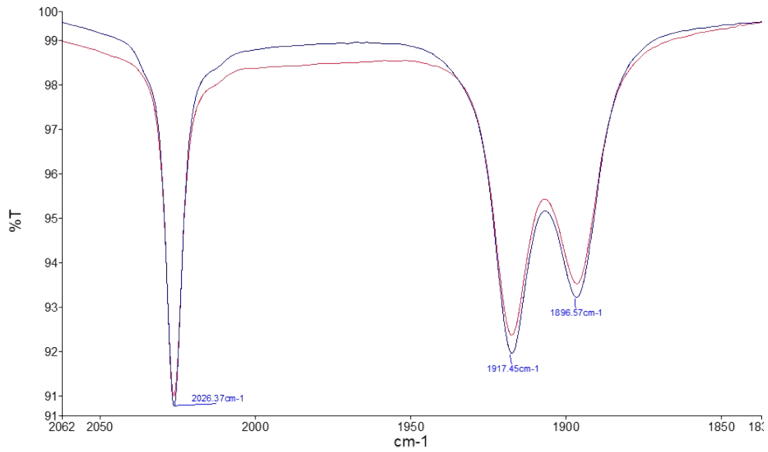

Figure S3: FTIR monitoring of the stability of complex **1** in CH_3CN solution (red trace after 2 minutes, blu trace after 4 h) at room temperature

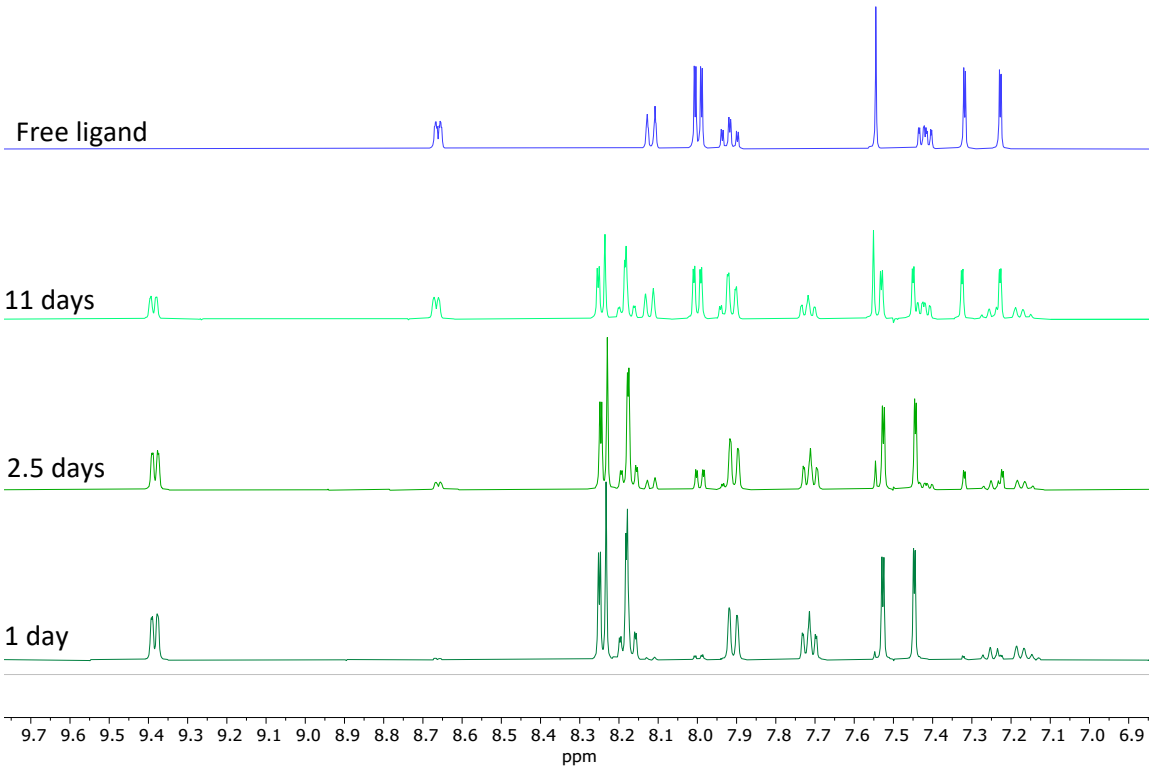

Figure S4: ^{1}H NMR monitoring of slow decomposition of **1** in DMSO-d_6 solution (300 K, 9.4 T). The upper trace reports the ^{1}H NMR spectrum of the free ligand in the same solvent.

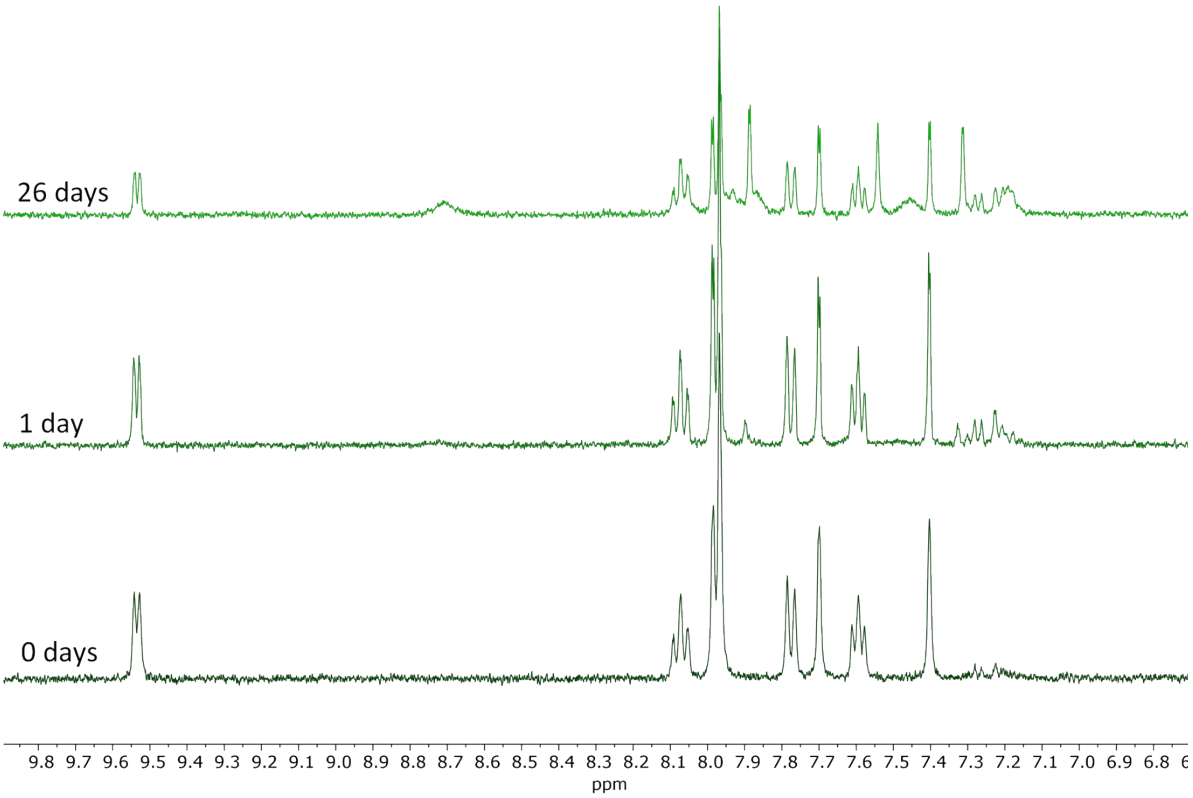

Figure S5: ^{1}H NMR monitoring of stability of complex **1** in CD_3CN solution (300 K, 9.4 T).

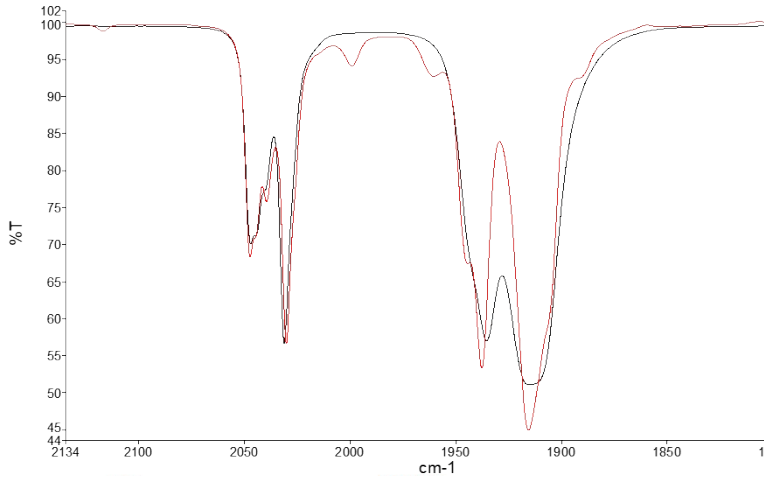

Figure S6: FTIR monitoring of stability of complex **2** in solid state, at room temperature. Red trace: freshly isolated complex **2**, black trace after one month.

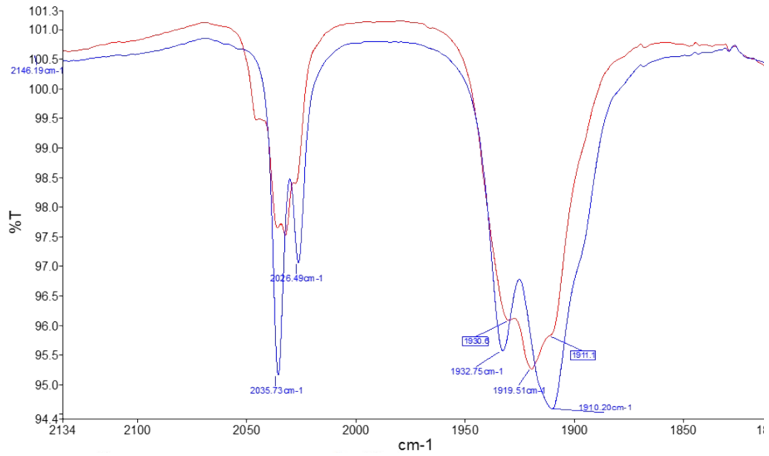

Figure S7: FTIR monitoring of the stability of complex **2** in CH_3CN solution (red trace after 2 minutes, blu trace after 10 minutes) at room temperature. $[ReCl(CO)_3(MeCN)_2]$ ν(CO) = 2035 s, 1932 s, 1910 s, cm^{-1}. Complex **1**: ν(CO) = 2026 s, 1917 s, 1896 s, cm^{-1} (the stretching at 1917 and 1896 cm^{-1} appear as shoulders of the more intense band of $[ReCl(CO)_3(MeCN)_2]$ centered at 1910 cm^{-1}).

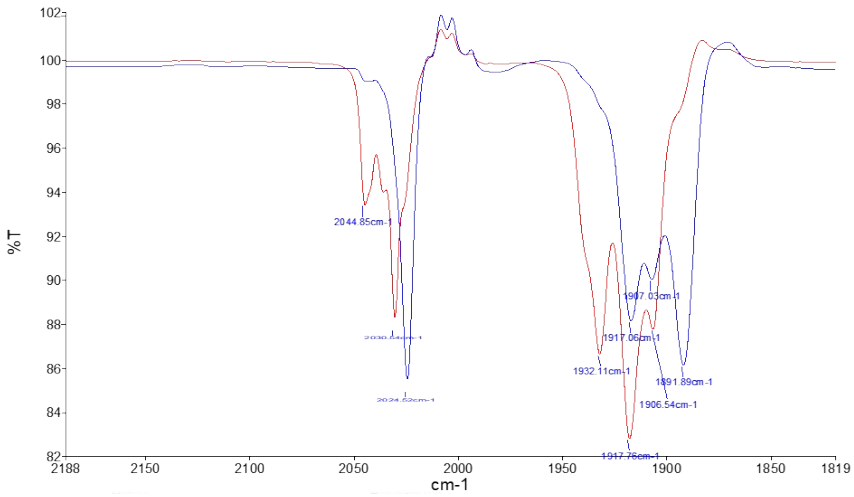

Figure S8: FTIR monitoring of the stability of complex **2** in THF solution (blue trace after 2 minutes, red trace after 10 minutes) at room temperature. $[ReCl(CO)_3(THF)_2]$ ν(CO) = 2024 s, 1906 s, 1891 s, cm^{-1}. Complex **1**: ν(CO) = 2024 s, 1917 s, 1891 s, cm^{-1} (the stretching at 2024 and 1891 cm^{-1} of $[ReCl(CO)_3(THF)_2]$ are overlapped to those of complex **1**).

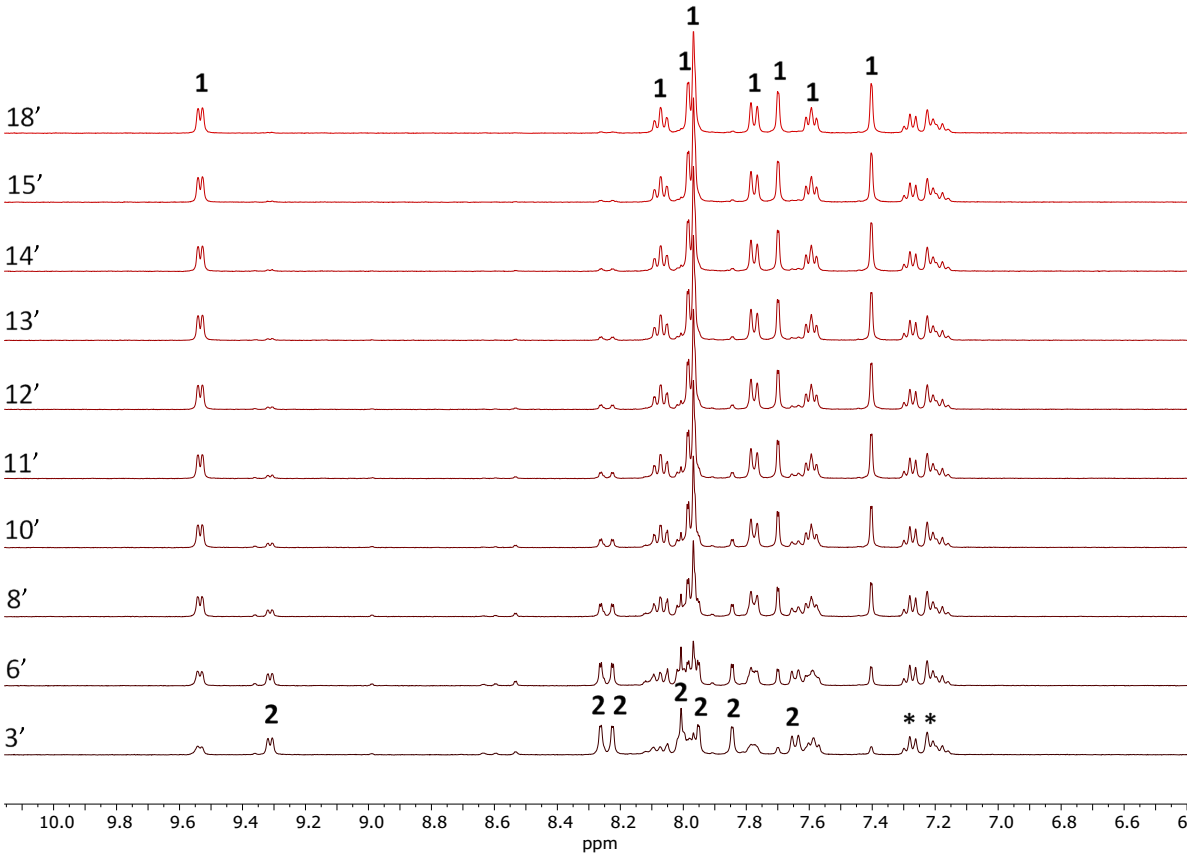

Figure S9: ^{1}H NMR monitoring of decomposition of **2** in CD_3CN solution (300 K, 9.4 T). After only 3 min complex **1** accounts for 38% of the mixture and it becomes 58% after 6 min. $t_{1/2}$ is = 5 min.

On the bases of position and splitting pattern, the most downfield shifted doublet is assigned to the CH(5') of the pyridine ring (9.38 ppm, dd, $^{3}J_{HH}$=5.8 Hz, $^{4}J_{HH}$=1.2 Hz). From this starting point, it is easy to assign the other pyridine signals, namely (CH(4') = 7.72 ppm, ddd $^{3}J_{HH}$=5.8 Hz, $^{3}J_{HH}$=7.65 Hz, $^{4}J_{HH}$=1.0 Hz; CH(3') = 8.2 ppm, ddd $^{3}J_{HH}$=5.8 Hz, $^{3}J_{HH}$=7.9 Hz, $^{4}J_{HH}$=1.2 Hz; CH(2') = 7.91 ppm, dd, $^{3}J_{HH}$=7.9 Hz, $^{4}J_{HH}$= 1.0 Hz).

CH(2) is an isolated spin and gives rise to a singlet signal centered at 8.23 ppm. Finally, the four signals of triimidazole ligand (6, 7, 10 and 11) give rise to 4 doublets, paired two by two: the two signals, labelled with Δ, at 8.25 ppm and 7.52 ppm ($^{3}J_{HH}$=2.0 Hz); and the two signals ,labelled with 🐟, at 8.18 ppm and 7.45 ppm ($^{3}J_{HH}$=1.7 Hz).

On the bases of the scalar couplings, it is not possible to assign these signals neither to the couples 6/7 and 10/11, nor discriminate between 6 and 7, or 10 and 11.

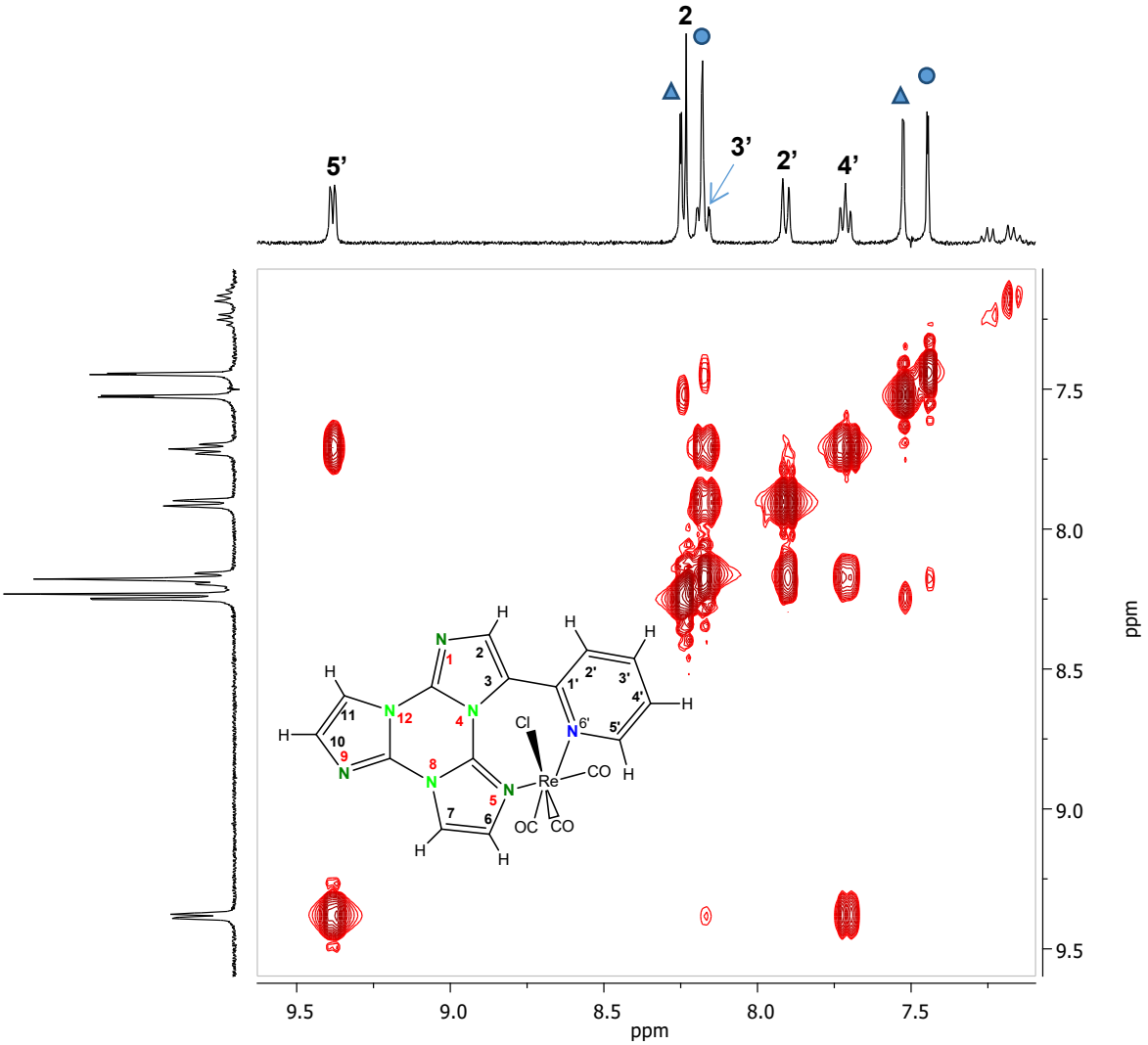

Figure S10. 2D ^{1}H COSY (homonuclear scalar correlation spectroscopy) NMR experiment of complex **1** in DMSO-d_6 (300 K, 9.4 T).

The shift upon coordination of N5 was fundamental to attribute the signal at 7.52 ppm to CH(6) of imidazole C ring . On the bases of this attribution, the resonance at 8.25 ppm was unequivocally attributed to CH(7) (see ^{1}H COSY experiment). For similarity, the resonance at 7.45 ppm was assigned to CH(10) and the signal at 8.18 ppm to CH(11).

As to the other N-H correlations of imidazole rings A and B, we can see from this experiment that N1 and N9 have pretty almost the same chemical shift (154.1 vs 154.3 ppm) and were attributed through their correlation with CH(2) of ring A and CH(10) and CH(11) of ring B. While these long range cross peaks were selected by a $^{2}J_{NH}$ scalar correlation, N4, N8 and N12 showed $^{3}J_{NH}$ scalar correlations with the CH of their same imidazole rings. Finally N6' showed also cross peaks of minor intensity with pyridine CH(4') and (2') in meta position.

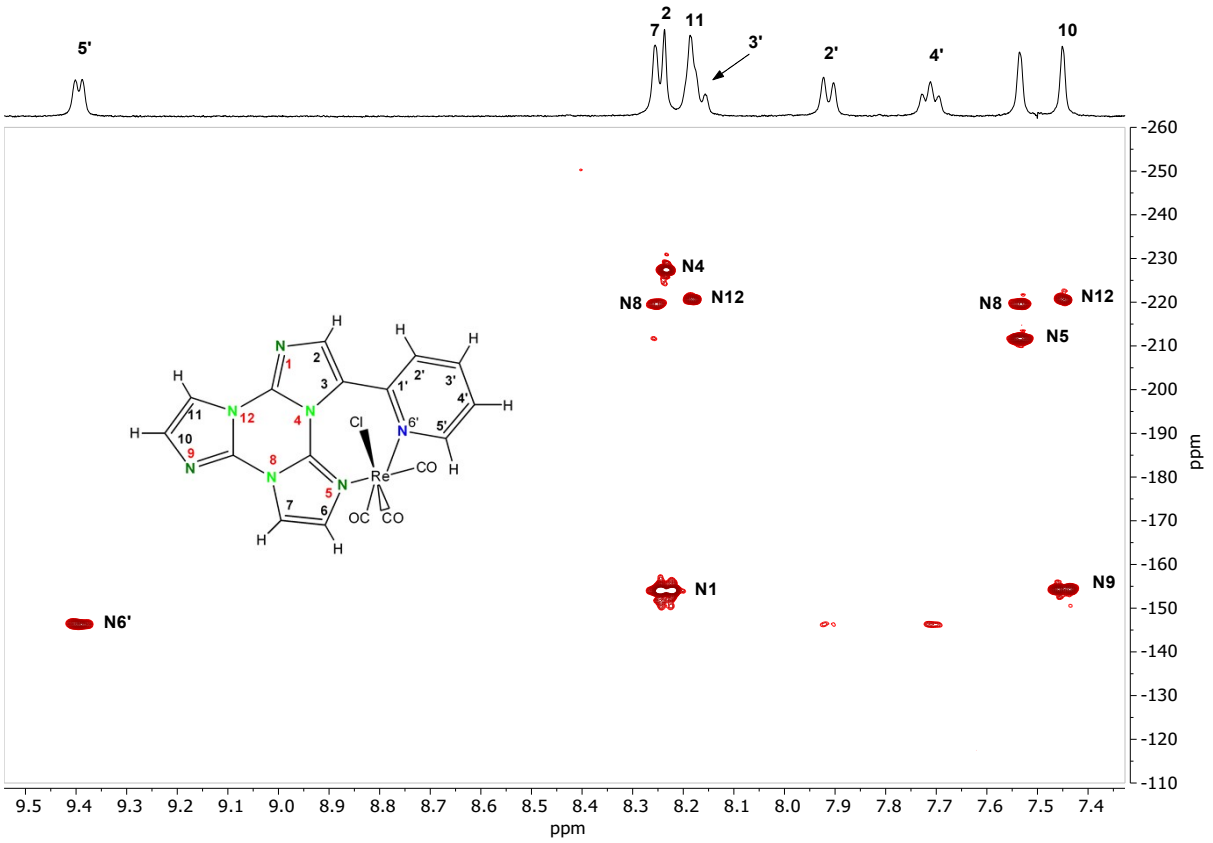

Figure S11. 2D ^{1}H-^{15}N HMBC (heteronuclear long-range scalar correlation spectroscopy) NMR experiment of complex **1** in DMSO-d_6 (300 K, 9.4 T).

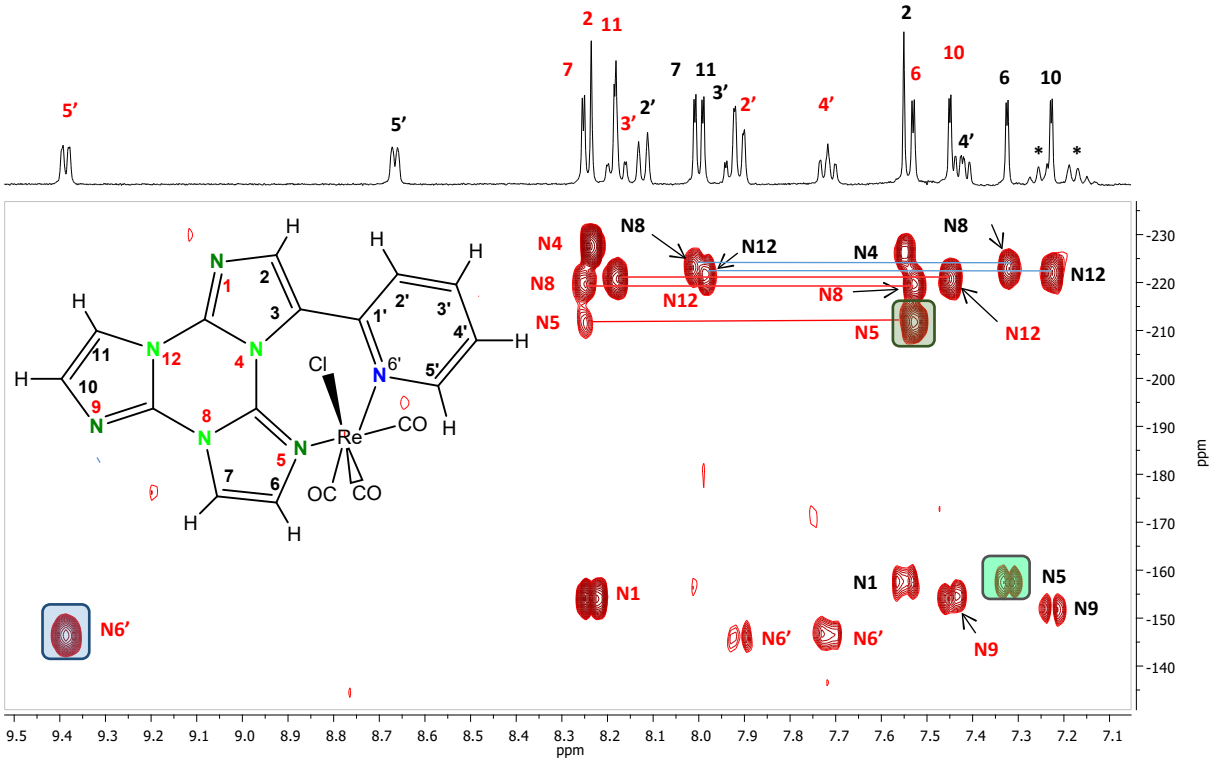

Figure S12. 2D ^{1}H-^{15}N HMBC (heteronuclear long-range scalar correlation spectroscopy) NMR experiment of a mixture of complex **1** (red labels) and free ligand **2-Py-TT** (black labels) in DMSO-d_6 (300 K, 9.4 T).

The experiment ^{1}H-^{13}C HSQC allowed the identification of all the CH signals of the complex **1**. The identification and attribution of all the quaternary carbons was achieved by a long range correlation experiment (see below).

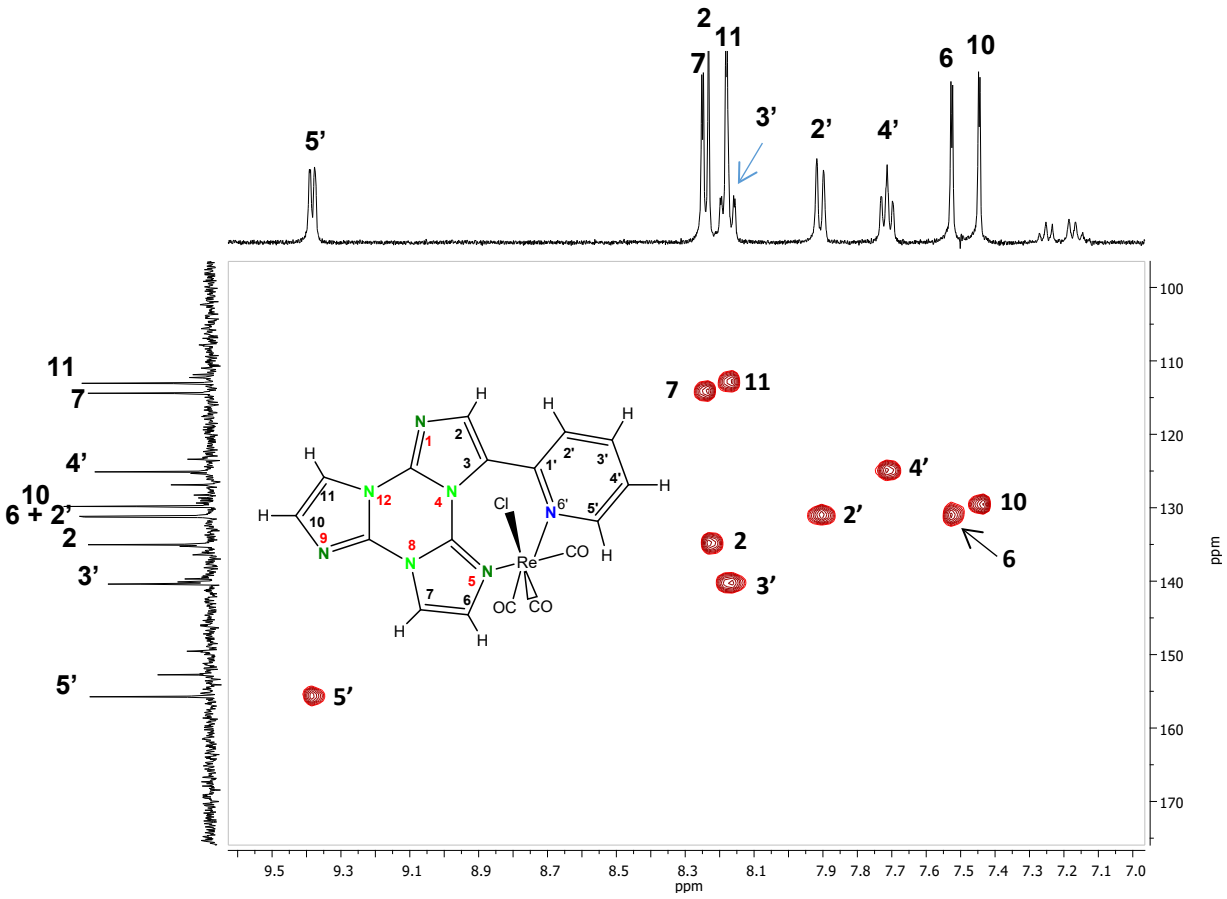

Figure S13. 2D ^{1}H-^{13}C HSQC (heteronuclear direct scalar correlation spectroscopy) NMR experiment of complex **1** in DMSO-d_6 (300 K, 9.4 T).

H(5') shows strong C-H long range correlations with carbons CH(4') and CH(3'), as well as with the quaternary C(1') lying at 152.8 ppm (highlighted by a blue box). The same quaternary atom correlates also with protons H(3') and H(2') of the pyridine ring.

The singlet H(2) was exploited for the identification of the quaternary carbons of imidazole ring A, C(3) and C(12a): since signal at 126.9 ppm correlates also with the pyridine signal H(2'), it was assigned to C(3). Hence, signal at 139.7 ppm was assigned to C(12a) (cross peaks are highlighted in yellow boxes).

Both CH signals of ring *B,* H(10) and H(11), show correlations (cross peaks highlighted in green) with the same quaternary signal at 135.3, assigned to C(8a).

Finally, CH signals of ring *C,* H(6) and H(7), show cross peaks (highlighted with the red boxes) with the quaternary resonance at 140.1 ppm (almost overlapped to CH(3') signal), assigned to C(4a).

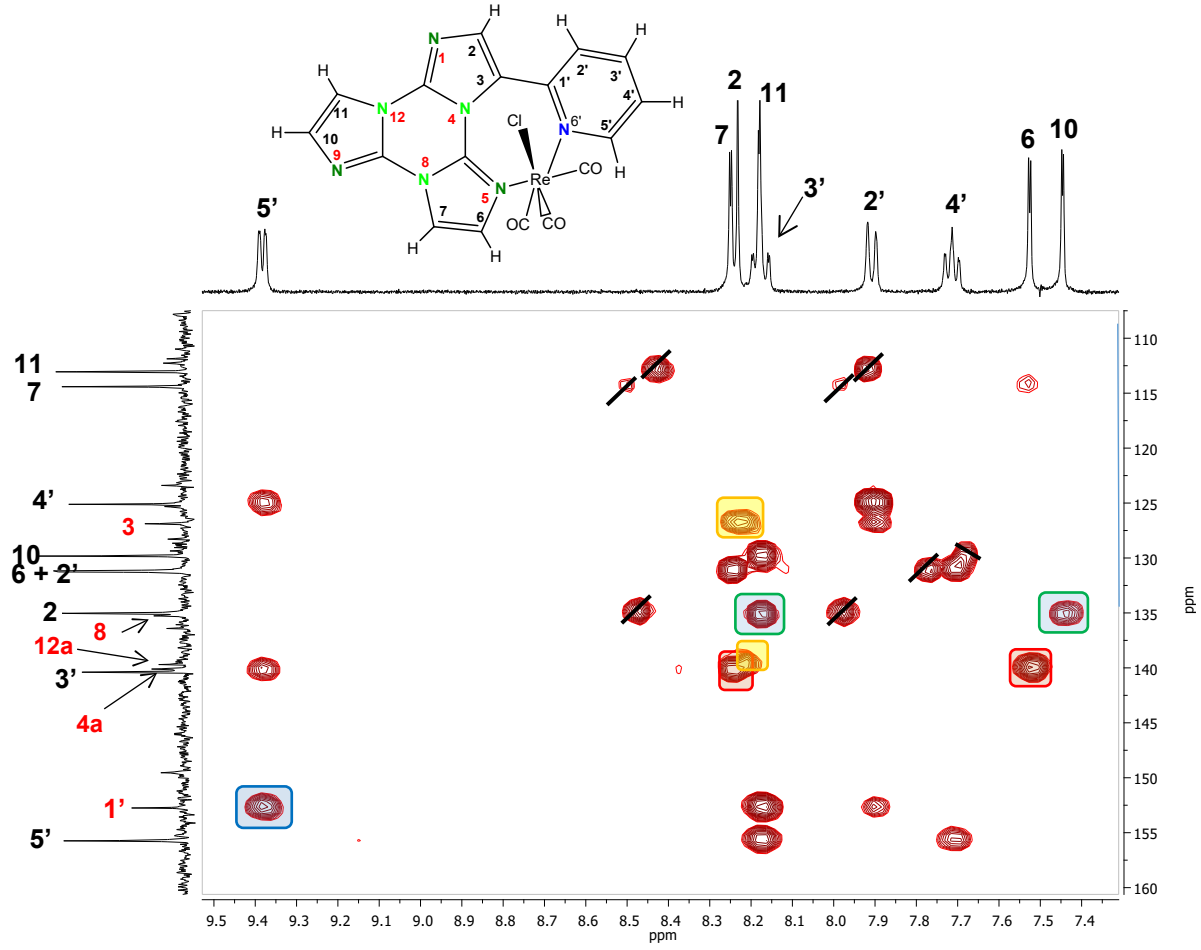

Figure S14. 2D ^{1}H-^{13}C HMBC (heteronuclear long-range scalar correlation spectroscopy) NMR experiment of complex **1** in DMSO-d_6 (300 K, 9.4 T). With black bars some correlation peaks due to direct CH coupling residues have been cancelled for the sake of clarity. The quaternary carbons have been highlighted with red labels on F1 axis.

Table S1. Experimental and calculated ^{1}H, ^{13}C and ^{15}N chemical shift of complex **1** and **TT-Py** in DMSO-d_6.

	Assignment	Complex 1 δppm (*DFT*)			TT-Py δppm (*DFT*)		
		^{1}H	^{13}C	^{15}N	^{1}H	^{13}C	^{15}N
Ring A	**N(1)**	---	---	-154.1 (*-164.6*)			-157.7 (*-169.4*)
	CH(2)	8.23 (*8.16*)	135.0 (*142.8*)	---	7.54 (*8.05*)	129.9 (*138.8*)	
	C(3)	---	126.9 (*133.7*)	---		128.4 (*136.4*)	
	C(12a)	---	139.7 (*142.6*)	---		137.4 (*141.5*)	
	N(4)	---	---	-227.4 (*-239.6*)			-226.3 (*-238.4*)
Ring C	**C(4a)**	---	140.1 (*141.0*)	---		136.1 (*140.1*)	
	N(5)	---	---	-211.6 (*-206.5*)			-157.3 (*-162.2*)
	CH(6)	7.52 (*7.70*)	131.2 (*138.0*)	---	7.32 (*7.55*)	129.1 (*134.6*)	
	CH(7)	8.25 (*8.16*)	114.2 (*118.6*)	---	8.01 (*8.15*)	112.3 (*116.5*)	
	N(8)	---	---	-219.7 (*-230.4*)			-211.5 (*-230.5*)
Ring B	**C8a**	---	135.3 (*138.4*)	---		136.4 (overlap with CH3') (*139.9*)	
	N9	---	---	-154.3 (*-164.8*)			-151.5 (*-169.9*)
	CH(10)	7.45 (*7.67*)	129.9 (*137.2*)	---	7.23 (*7.58*)	128.4 (*136.1*)	
	CH(11)	8.18 (*8.23*)	112.9 (*118.6*)	---	7.99 (*8.19*)	111.9 (*117.7*)	
	N(12)	---	---	-220.8 (*-231.2*)			-221-5 (*-232.4*)
Py Ring	**C1'**	---	152.8 (*157.2*)	---	---	147.8 (*153.9*)	
	C(H2')	7.91 (*8.02*)	131.2 (*137.7*)	---	8.12 (*8.95*)	125.3 (*131.4*)	
	C(H3')	8.20 (*8.26*)	140.4 (*146.9*)	---	7.92 (*8.33*)	136.4 (*143.0*)	
	C(H4')	7.72(*7.71*)	125.0 (*130.1*)	---	7.42 (*7.72*)	123.3 (*128.8*)	
	C(H5')	9.38 (*9.59*)	155.8 (*161.8*)	---	8.66 (*9.01*)	149.5 (*156.5*)	
	N6'	---	---	-146.8 (*-143.5*)			-68 (*-84.6*)

Table S2. Natural charges [*e*] computed in dimethyl sulfoxide for the hydrogen atoms of the free ligand **TT-Py** and the mononuclear complex **1**

	TT-Py	**1**
H2	0.281	0.289
H6	0.278	0.257
H7	0.280	0.303
H10	0.278	0.285
H11	0.277	0.281
H3′	0.264	0.286
H4′	0.271	0.294
H5′	0.262	0.276
H6′	0.265	0.210

The ^{1}H COSY experiment allowed the prompt identification of the four CH pyridine signals and their attribution, starting from CH(5') which is downfield shifted by the closeness to the heteroatom N6'. As far as the attribution of the signals of imidazole rings is concerned, with this experiment we were able to find couples of signals of CH lying on the same ring (indicated with the blue symbols Δ and 🕶), but as in the case of complex 1 this experiment was unable to assign these resonances. Resonance of the isolated CH(2) is accidentally overlapped to the toluene signals, as confirmed by the ^{1}H-^{13}C HMQC experiment (see below).

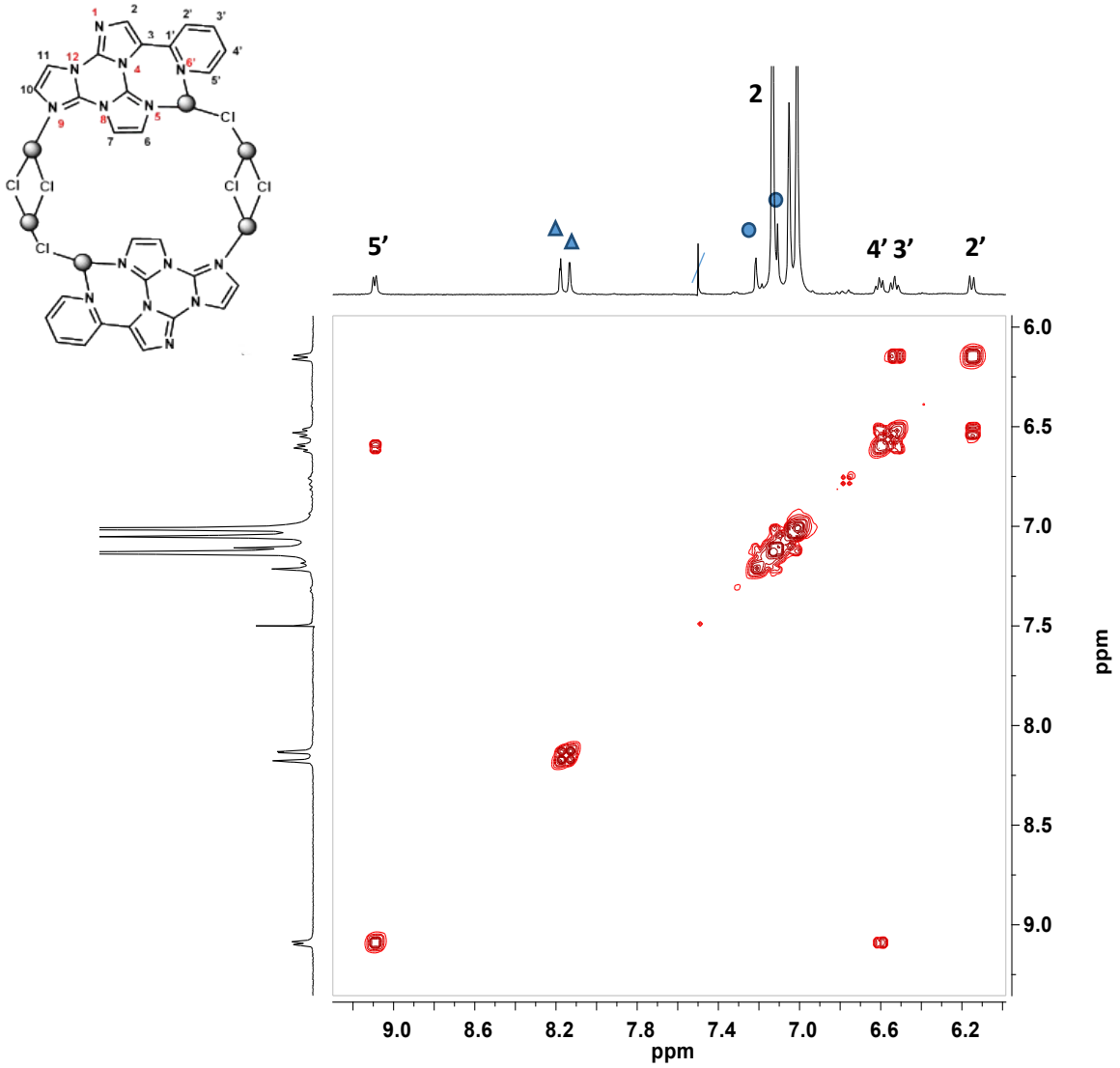

Figure S15. 2D ^{1}H COSY (homonuclear scalar correlation spectroscopy) NMR experiment of complex **2** in toluene-d_8 (300 K, 9.4 T).

As for complex **1**, also for complex **2** the ^{1}H-^{13}C direct scalar correlation spectroscopy was not enough for the assignment of the two couples of imidazole CH signals 6/7 and 10/11. Anyhow, this experiment allowed the attribution of all the other CH signals, and especially was crucial to highlight the presence of a CH signal completely overlapped to a toluene resonance (see cross peak at 7.13-112.95 ppm).

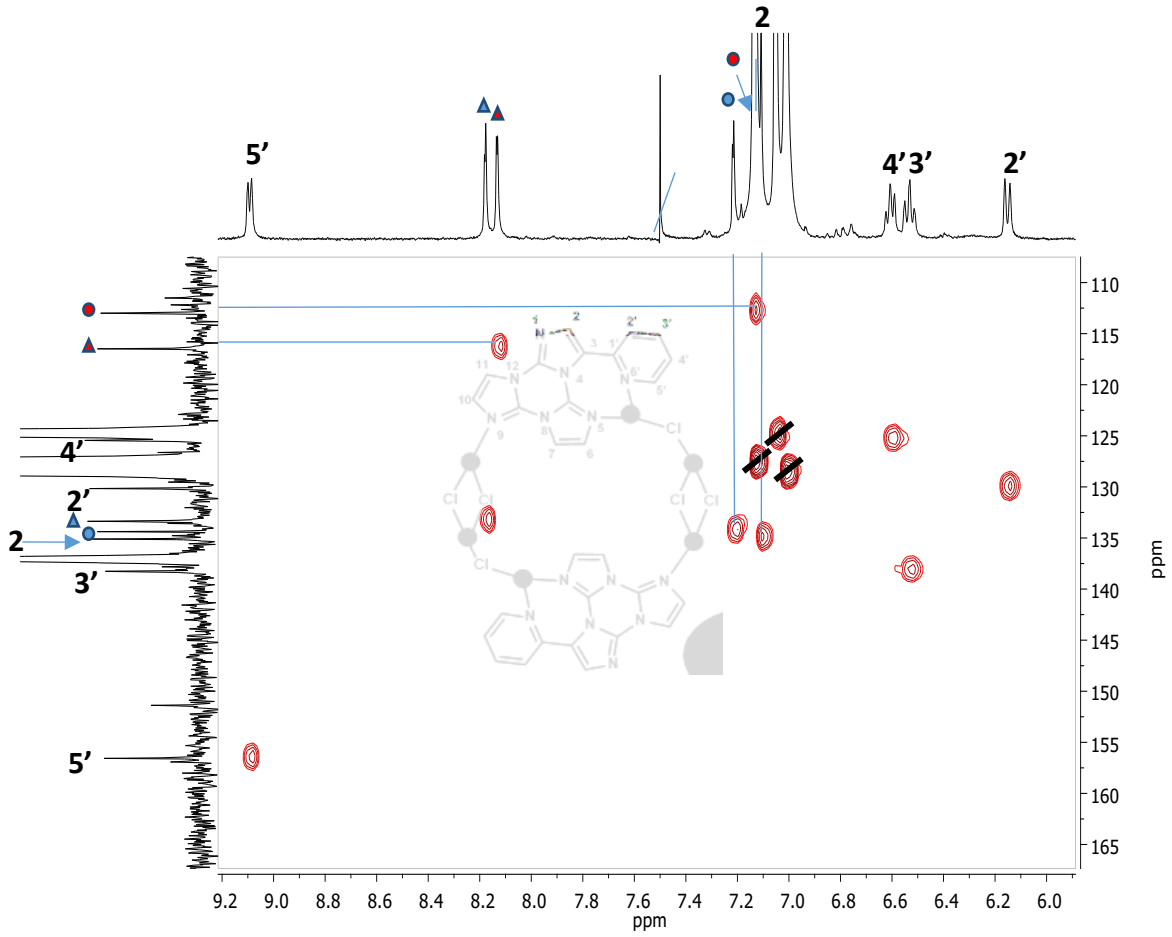

Figure S16. 2D ^{1}H-^{13}C HSQC (heteronuclear direct scalar correlation spectroscopy) NMR experiment of complex **2** in toluene-d_8 (300 K, 9.4 T).

This ^{1}H-^{15}N heteronuclear long-range scalar correlation was crucial to assign the resonances of the CH 6/7 and 10/11. Starting from the downfield shifted signal H5', it correlates with the pyridine N6' at -147.4 ppm. H2 individuates the imidazole N1 of ring A lying at -149.8 ppm ($^{2}J_{HN}$) and N4 of the same ring at -230.8 ppm ($^{3}J_{HN}$). As for imidazole ring A, one of the CH of ring B shows correlations with both its nitrogen atoms N9 and N12. For analogy with ring A, we attributed the proton lying at 8.13 ppm and showing these two last correlations to the H10. On the contrary, H11 shows a correlation with only N12 ($^{2}J_{HN}$). Similarly, proton signals of ring C were assigned considering that one of the two CH, lying at 7.22 ppm, shows two correlations with both N5 and N8, and hence it was assigned to H6, and consequently the H7 signal was attributed to the hidden signal at 7.13 ppm overlapped to one of the toluene signals.

In the case of complex **2**, the ^{15}N signals of TT moiety affected by coordination are two: N5 as in the case of complex **1**, and in addition N9.

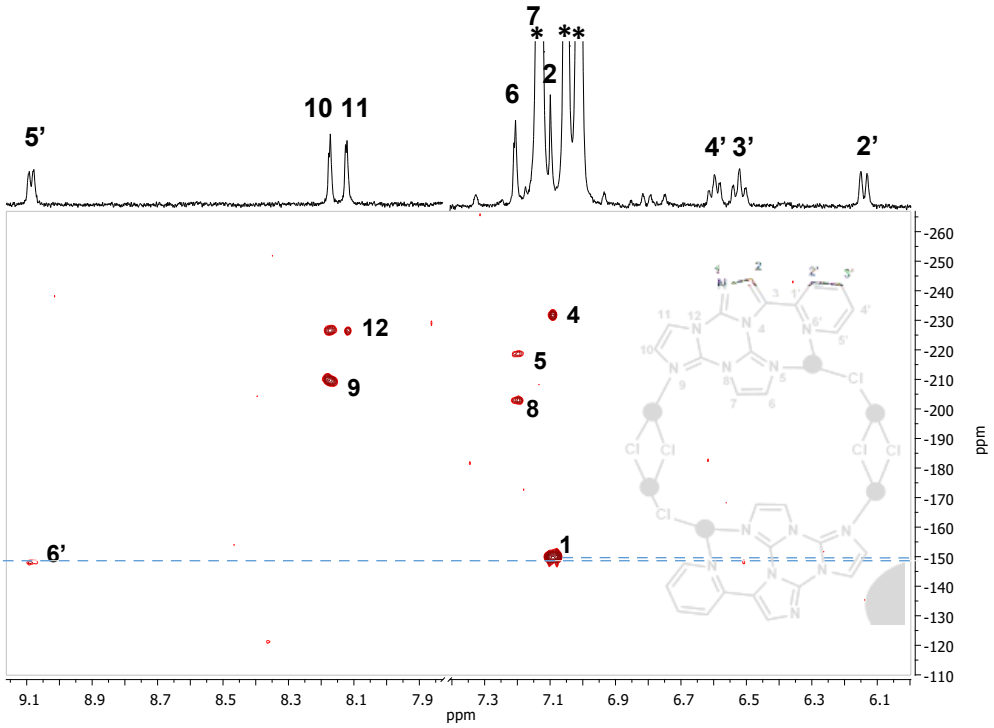

Figure S17. 2D ^{1}H-^{15}N HMBC (heteronuclear long-range scalar correlation spectroscopy) NMR experiment of complex **2** in toluene-d_8 (300 K, 9.4 T).

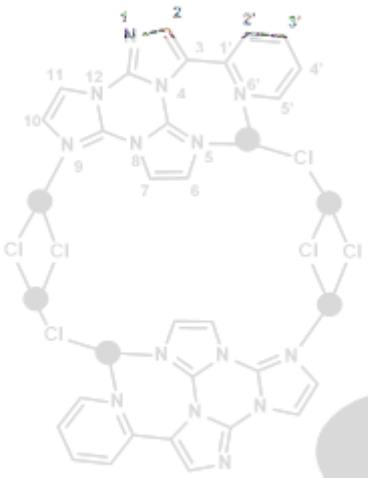

The ^{1}H-^{13}C heteronuclear long-range scalar correlation was carried out to attribute the quaternary carbons with the exception of carbonyl resonances. In black the CH resonances attributed on the bases of the direct C-H correlations (see Figure S8), indicating also the CH 6/7 and 10/11 attributed on the bases of NH long range correlation experiment (see Figure S9) have been labelled here. All these assignments were coherent with the long range correlations shown by this experiment. H5' shows, apart the long range correlations with pyridine CH(4') and CH(3'), also with the quaternary carbon C1' at 151.3 ppm. Moreover, this last one shows strong long range correlations also with H3' and H2'. Both H6 and H7 of ring C show long range correlations with quaternary carbon 4a, while H10 and H11 of ring B not only show correlations with the quaternary carbon 8a of their imidazole ring, but H11 show a correlation with a quaternary carbon 12a of ring A. The only C_q peak that cannot be found by this experiment is the C3, since neither H2 nor H2' develop visible cross peaks.

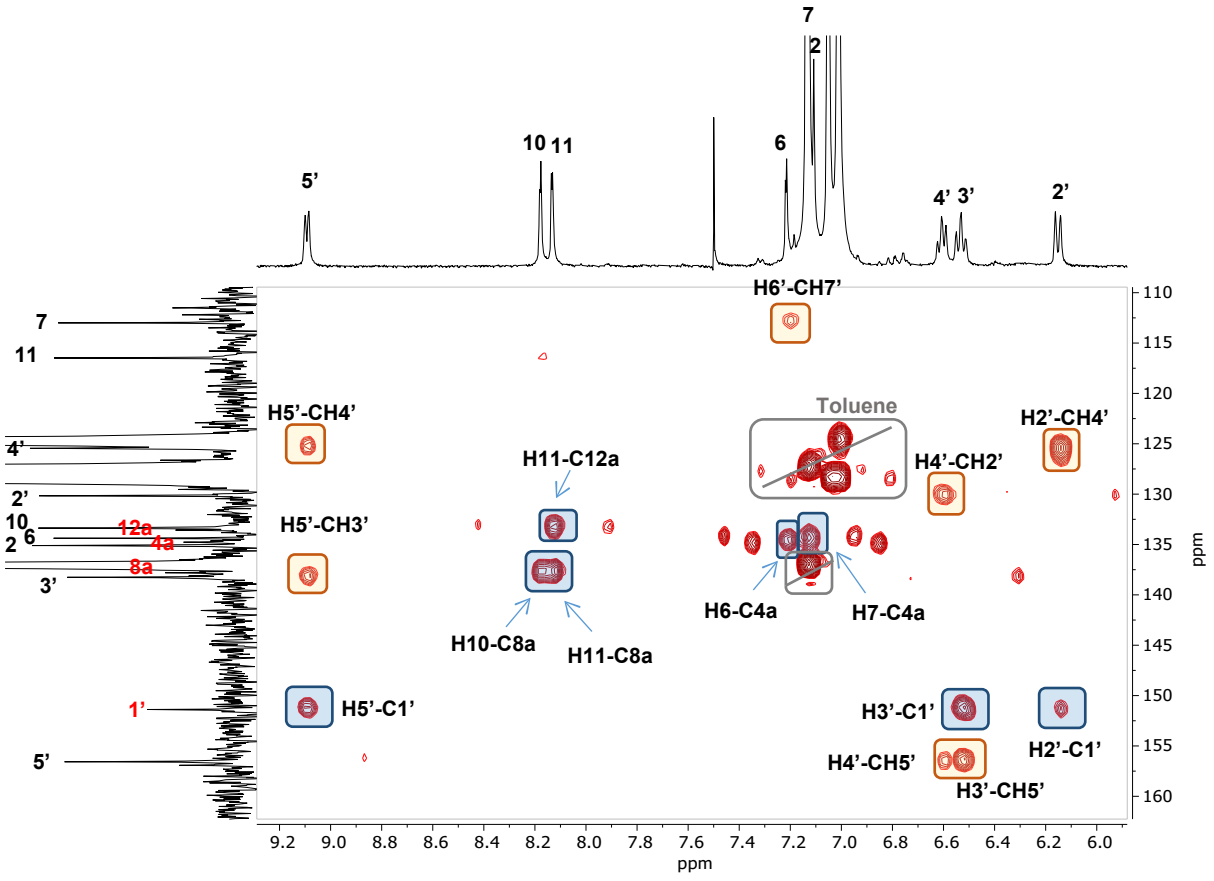

Figure S18. 2D ^{1}H-^{13}C HMBC (heteronuclear long-range scalar correlation spectroscopy) NMR experiment of a mixture of complex **2** in toluene-d_8 (300 K, 9.4 T). Long range correlations that individuate a quaternary carbon are highlighted in the blue box, while the long range correlations between CH groups are highlighted in orange. The remaining cross peaks are due to direct correlations residues that appeared as ^{13}C satellites of ^{1}H signals, since the coupling with the 1.1% ^{13}C was not totally cancelled.

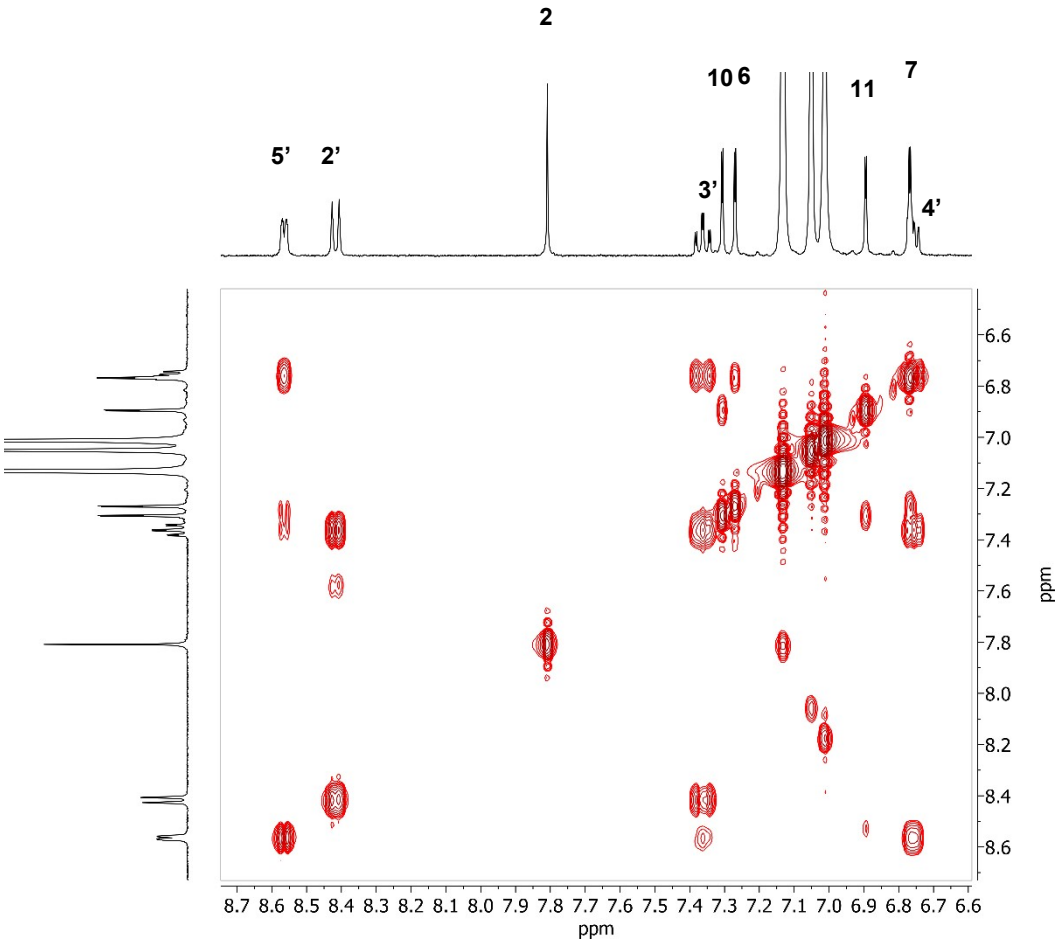

Figure S19. ^{1}H COSY (toluene-d_8, 300 K, 9.4 T) of the free ligand **TT-Py**.

From the diffusion coefficients measured by diffusion ordered spectroscopy for complex **2** (D_t = 708 μm^2/s) resulted lower than for complex **1** (D_t = 891 μm^2/s), which is visible as very minor component of this sample and derives from a starting decomposition of complex **2**.

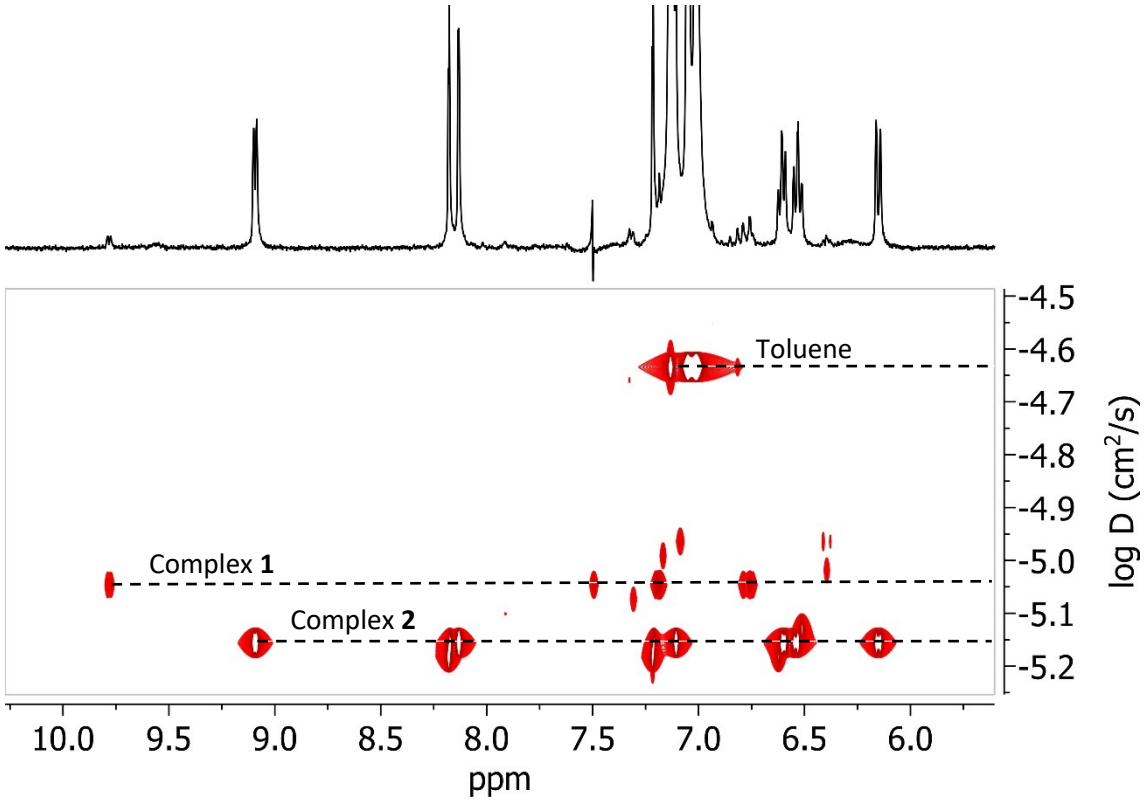

Figure S20. ^{1}H 2D DOSY of a sample of complex **2** containing a very small amount of complex **1**, which is mostly insoluble in toluene-d_8 (300 K, 9.4 T, δ = 2 ms, Δ = 100 ms).

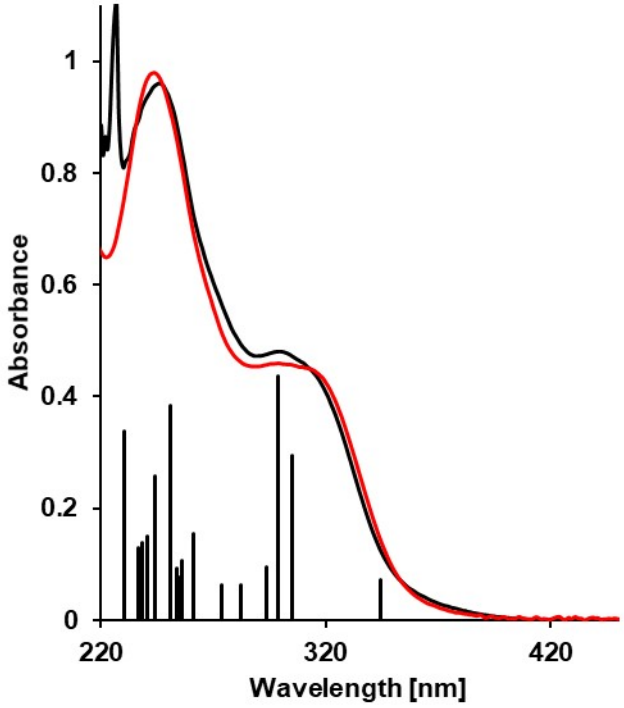

Figure S21. Absorption spectra of complex **1** in CH_2Cl_2 (black trace) and MeCN (red trace). Samples are measured at room temperature. A comparison with excitation energies and oscillator strengths (vertical black lines) computed in dichloromethane is reported.

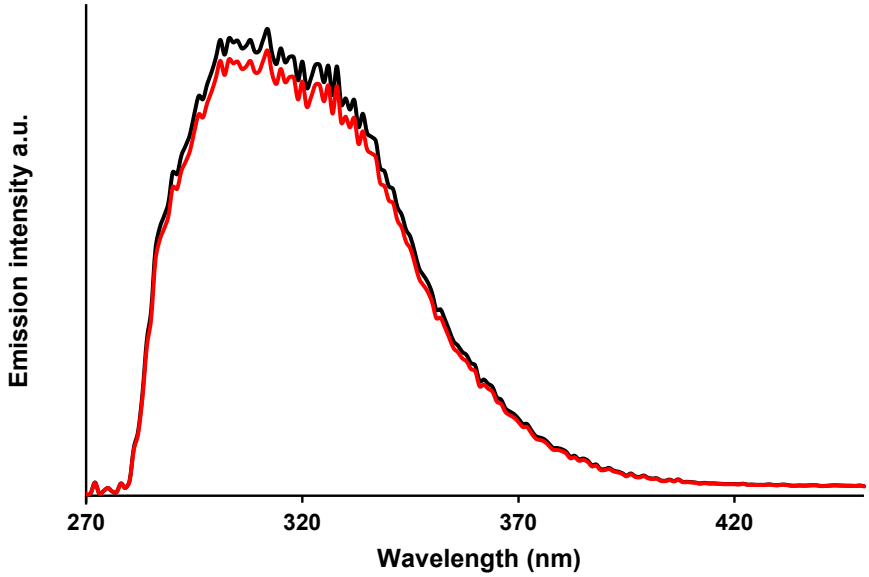

Figure S22: Excitation spectra of **1**(black trace) and **2** (red trace) in toluene solution at room temperature

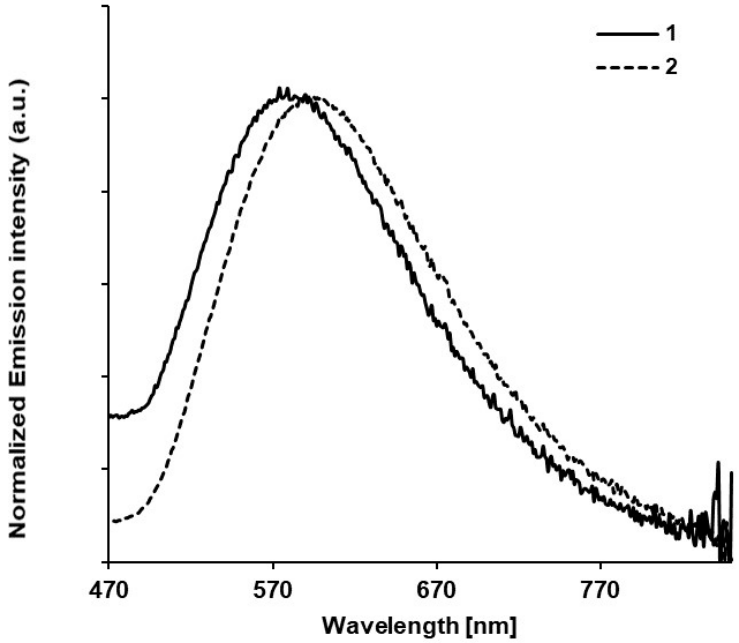

Figure S23. Emission spectra of **1** and **2** in solid state at 298 K upon excitation at 365 nm.

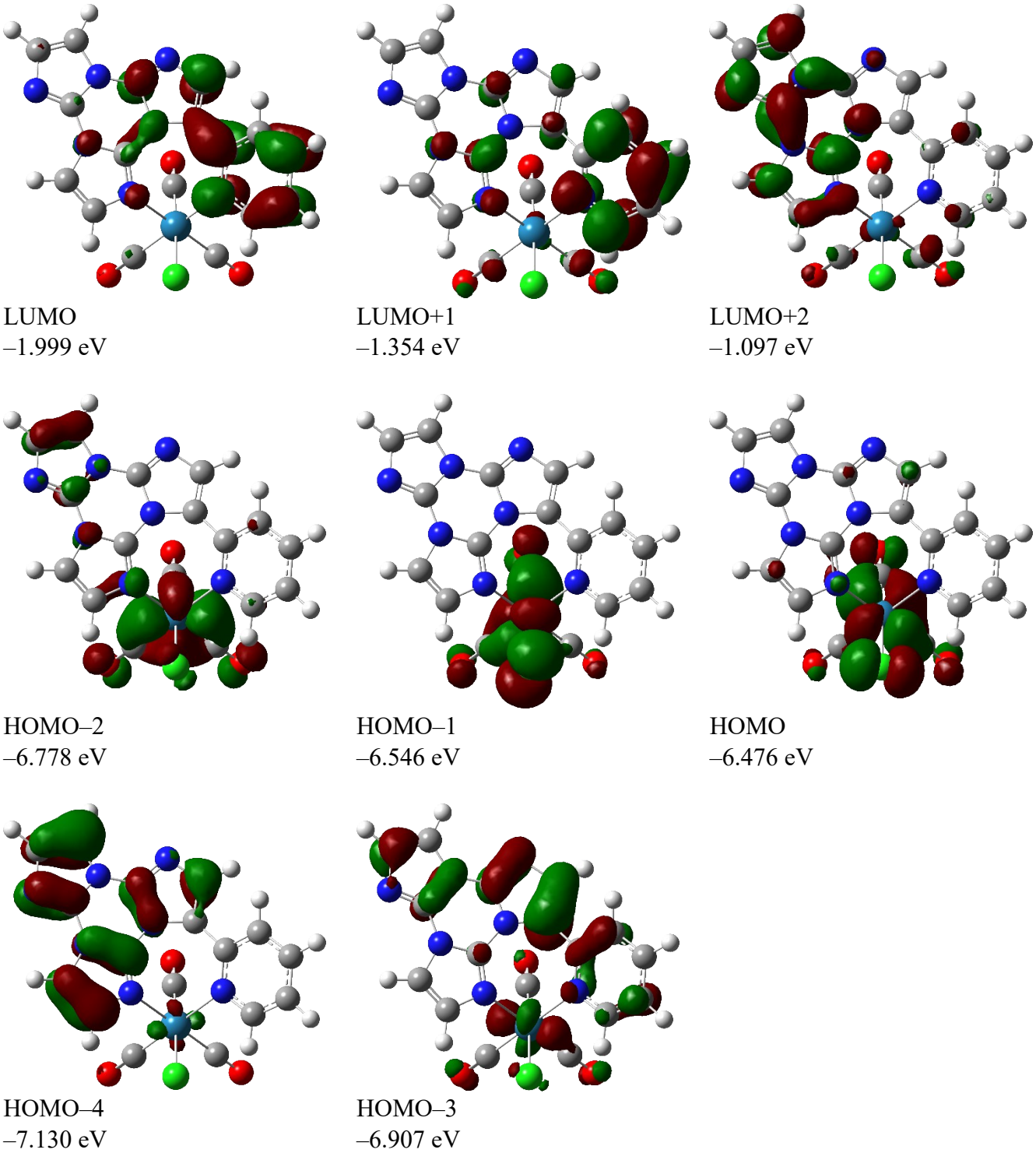

Figure S24. Isodensity surface plots and energies computed for some relevant molecular orbitals of *fac*-[Re(TT-Py)(CO)$_3$Cl] (**1**), as computed in dichloromethane.

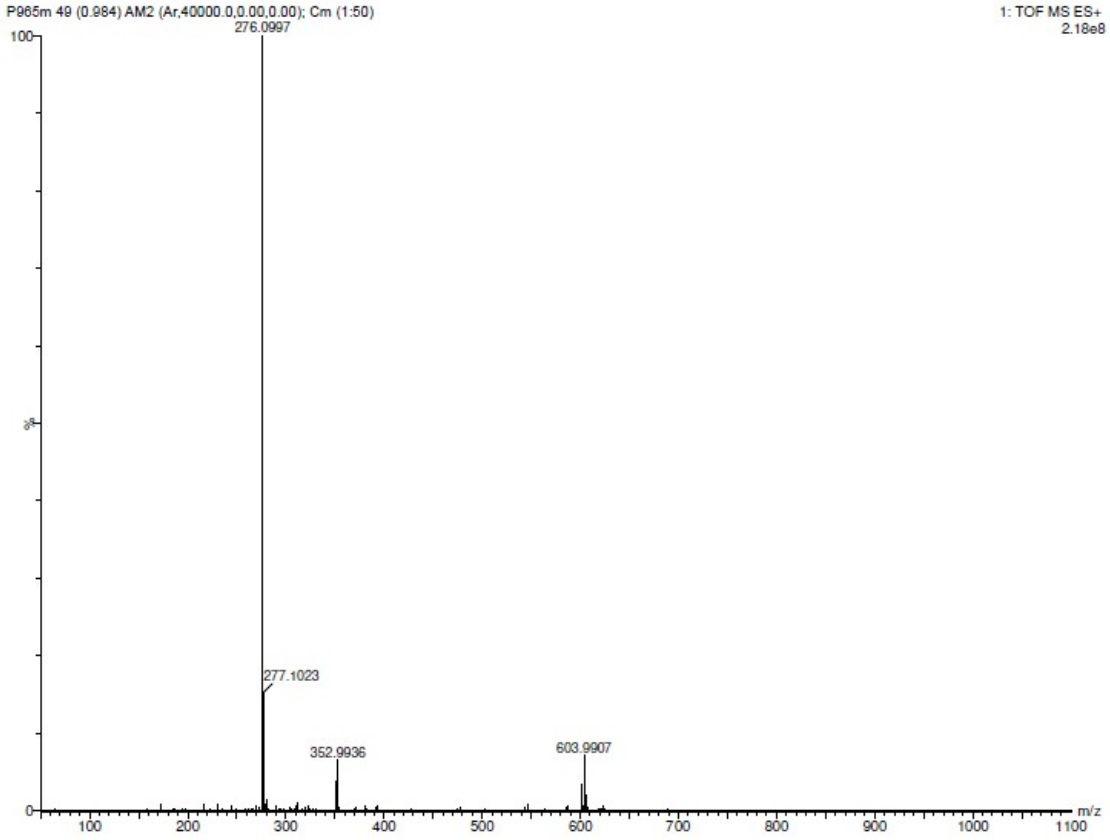

Figure S25. Mass analysis of complex **1**

Table S3. Selected bond distances [Å] and angles [°] for the rhenium complexes **1** and **2**

1		**2**			
Re1–Cl1	2.4808(4)	Re1–Cl1	2.539(3)	Re4–Cl4	2.516(3)
Re1–C1	1.9079(15)	Re1–C1	1.899(16)	Re4–C24	1.909(13)
Re1–C2	1.9192(16)	Re1–C2	1.914(14)	Re4–C25	1.919(15)
Re1–C3	1.9116(14)	Re1–C3	1.919(17)	Re4–C26	1.916(15)
Re1–N3	2.1855(11)	Re1–N3	2.182(11)	Re4–N10	2.186(10)
Re1–N7	2.2169(11)	Re1–N7	2.208(12)	Re4–N14	2.208(12)
Cl1–Re1–C1	176.26(5)	Cl1–Re1–C1	177.6(5)	Cl4–Re4–C24	179.3(4)
Cl1–Re1–C2	93.12(5)	Cl1–Re1–C2	95.9(5)	Cl4–Re4–C25	93.2(4)
Cl1–Re1–C3	94.22(4)	Cl1–Re1–C3	92.2(4)	Cl4–Re4–C26	88.3(4)
Cl1–Re1–N3	82.82(3)	Cl1–Re1–N3	82.4(3)	Cl4–Re4–N10	84.2(3)
Cl1–Re1–N7	84.51(3)	Cl1–Re1–N7	86.9(3)	Cl4–Re4–N14	87.4(3)
C1–Re1–C2	89.26(7)	C1–Re1–C2	86.4(7)	C24–Re4–C25	87.4(6)
C1–Re1–C3	88.66(6)	C1–Re1–C3	88.7(7)	C24–Re4–C26	92.1(6)
C1–Re1–N3	94.79(5)	C1–Re1–N3	95.4(6)	C24–Re4–N10	95.2(5)
C1–Re1–N7	92.52(5)	C1–Re1–N7	92.1(6)	C24–Re4–N14	92.2(5)
C2–Re1–C3	89.72(7)	C2–Re1–C3	87.9(6)	C25–Re4–C26	86.4(7)
C2–Re1–N3	175.95(6)	C2–Re1–N3	176.5(5)	C25–Re4–N10	177.2(5)
C2–Re1–N7	92.32(6)	C2–Re1–N7	94.3(5)	C25–Re4–N14	92.0(6)
C3–Re1–N3	90.47(5)	C3–Re1–N3	89.1(5)	C26–Re4–N10	92.6(5)
C3–Re1–N7	177.66(5)	C3–Re1–N7	177.7(5)	C26–Re4–N14	175.3(5)
N3–Re1–N7	87.41(4)	N3–Re1–N7	88.7(4)	N10–Re4–N14	88.8(4)

Table S4. Properties of some of the more intense electronic transitions computed for *fac*-[Re(TT-Py)(CO)$_3$Cl] (**1**) in dichloromethane.

S_n	E [eV]	λ [nm]	f		
S_4	4.061	305	0.1336	HOMO→LUMO+1	32%
				HOMO–3→LUMO	56%
S_5	4.147	299	0.1983	HOMO→LUMO+1	46%
				HOMO–3→LUMO	25%
S_{19}	4.937	251	0.1746	HOMO–3→LUMO+2	50%
				HOMO–4→LUMO+1	13%
S_{21}	5.081	244	0.1171	HOMO–3→LUMO+2	12%
				HOMO–4→LUMO+1	48%

Table S5. Properties of the lowest lying triplets computed for *fac*-[Re(TT-Py)(CO)$_3$Cl] (**1**) in toluene.

T_n	E [eV]	λ [nm]		
T_1	2.897	428	HOMO→LUMO	22%
			HOMO–3→LUMO	51%
T_2	3.268	379	HOMO–1→LUMO	73%
T_3	3.345	371	HOMO→LUMO	66%
			HOMO–3→LUMO	16%
T_4	3.480	356	HOMO–1→LUMO	15%
			HOMO–2→LUMO	63%

Computational details. Ground state geometries of the free ligand **TT-Py** and the mononuclear complex **1** were optimized by means of density functional calculations. The parameter-free hybrid functional PBE0[1] was employed along with the standard valence double-ζ polarized basis set 6-31G(d,p) for C, H, N and O. For Re the Stuttgart–Dresden effective core potentials were employed along with the corresponding valence triple- ζ basis set. All the calculations were done in the presence of solvent (dimethyl sulfoxide, used in the NMR characterizations, dichloromethane and toluene, used in the photophysical characterization) described by a polarizable continuum model (PCM).[2] The nature of all the stationary points was checked by computing vibrational frequencies and all the geometries were found to be true minima.
Structures optimized in dimethyl sulfoxide were used to predict NMR shielding tensors for ^{1}H, ^{13}C and ^{15}N according to the Gauge-Independent Atomic Orbital (GIAO) method,[3] employing the PBE0 functional and the standard valence triple-ζ polarized basis set 6-311++G(d,p) for C, H, N and O. Chemical shifts were referenced to the values computed at the same level of theory for tetramethylsilane in trichloromethane (for ^{1}H and ^{13}C) and neat nitromethane (for ^{15}N).[4]
The structure optimized in dichloromethane was used to simulate the absorption electronic spectrum of **1** down to 225 nm, computing the lowest 30 singlet excitation energies by means of time-dependent density functional calculations. The structure optimized in toluene was used to compute the lowest lying triplet excitation energies by means of time-dependent density functional calculations.
All the calculations were done with Gaussian 16.[5]

References

1 Called PBE1PBE in Gaussian. C. Adamo and V. Barone "Toward reliable density functional methods without adjustable parameters: The PBE0 model" *J. Chem. Phys.* 1999, **111**, 6158–6170. 10.1063/1.478522

2 G. Scalmani and M.J. Frisch "Continuous surface charge polarizable continuum models of solvation. I. General formalism" *J. Chem. Phys.* 2010, **132**, 114110-1–15. 10.1063/1.3359469

3 K. Wolinski, J. F. Hilton and P. Pulay "Efficient implementation of the Gauge-Independent Atomic Orbital method for NMR chemical shift calculations" *J. Am. Chem. Soc.*, 1990, **112**, 8251–8260. 10.1021/ja00179a005

4 R.K. Harris, E.D. Becker, S.M. Cabral De Menezes, R. Goodfellow and P. Granger "NMR nomenclature. Nuclear spin properties and conventions for chemical shifts" *Pure Appl. Chem.* 2001, **73**, 1795–1818. 10.1351/pac200173111795

5 Gaussian 16 (revision A.03), Gaussian Inc., Wallingford, CT, 2016. gaussian.com